

The influence of reflectivity color on Gabor deconvolution

Peng Cheng

CREWES, University of Calgary, Calgary, Alberta, Canada

chengp@ucalgary.ca

and

Gary F. Margrave

CREWES, University of Calgary, Calgary, Alberta, Canada

margrave@ucalgary.ca

Summary

We analyze the influence of nonwhite reflectivity on Gabor deconvolution. Testing on synthetic data shows that large phase rotations and amplitude distortions occur when reflectivity color is ignored and can be attributed to reflectivity's spectral color and temporal color respectively.

Introduction

There are various deconvolution methods, such as conventional wiener spiking deconvolution and Gabor deconvolution (Margrave and Lamoureux, 2002). Generally, the results are imperfect. This means that the estimation gives imperfect relative amplitude estimation, and there is an apparent phase shift between the deconvolved result and a zero-phase synthetic seismic trace created from a well log. This imperfection can be attributed to noise and the imperfect wavelet estimation. In addition, deconvolution algorithms usually assume that the reflectivity is white. However, in practice, the reflectivity is colored, and the nonwhite reflectivity assumption can also produce distorted estimation. Cheng and Margrave (2009) proposed a color correction method for Gabor deconvolution, which gives improved estimation with better relative amplitude and smaller phase rotation. This reveals that the reflectivity color can cause distorted estimation. In the Gabor transform domain, the amplitude spectrum of nonwhite reflectivity shows a dependency on both time and frequency, which we refer as temporal and spectral color. To distinguish the particular effect of temporal color and spectral color on Gabor deconvolution, further investigation should be conducted, which is the work of this paper.

Color correction and phase rotation

Cheng and Margrave (2009) proposed a color correction for Gabor deconvolution formulated in Gabor domain as following

$$R_G(\tau, f)_{est} = \frac{S_G(\tau, f) \overline{|R_G(\tau, f)|}}{|\overline{S_G(\tau, f)}| + \mu A_{max}} e^{i\varphi_c(\tau, f)}, \quad (1)$$

where $S_G(\tau, f)$ is the Gabor spectrum of seismic trace, $R_G(\tau, f)$ is the Gabor spectrum of the reflectivity calculated from the reference well log, μ is the stability factor, A_{max} is the maximum value of $|\overline{S_G(\tau, f)}|$, and $\varphi_c(\tau, f)$ is given by the Hilbert transform (over frequency)

$$\varphi_c(\tau, f) = H(\ln|\frac{\overline{|R_G(\tau, f)|}}{|\overline{S_G(\tau, f)}| + \mu A_{max}}|). \quad (2)$$

where H denotes the Hilbert transform. The conventional Gabor deconvolution (Margrave and Lamoureux, 2002) assumes that the reflectivity is white, i.e. $\overline{|R_G(\tau, f)|}$ is nearly constant. When the real $\overline{|R_G(\tau, f)|}$ demonstrates obvious spectral or temporal color feature (i.e. an apparent dependence on frequency or time), a white estimation tends to have distorted relative amplitude and large phase rotation compared with true reflectivity. The relative amplitude can be revealed

by comparing the envelopes of the estimated reflectivity and the true reflectivity calculated from well log. A simple way to roughly estimate the envelope of a signal $s(t)$ is formulated as

$$s_E(t) = \sqrt{s(t)^2 + s_H(t)^2}, \quad (3)$$

where $s_H(t)$ is the Hilbert transform of $s(t)$.

A definition of the nonstationary phase rotation was proposed by Cheng and Margrave (2009) as

$$s_\theta(t) = s(t)\cos(\theta(t)) + s_H(t)\sin(\theta(t)), \quad (4)$$

where $\theta(t)$ is the time-variant phase rotation, $s_H(t)$ is the Hilbert transform of $s(t)$, and $s_\theta(t)$ is the nonstationary phase rotated version of $s(t)$. The time-variant phase rotation between two signal $s_1(t)$ and $s_2(t)$ can be measured through least square analysis

$$\theta(t) = \min \|\{w(\tau - t)s_1(\tau)\}_\theta - w(\tau - t)s_2(\tau)\|, \quad (5)$$

where $w(\tau - t)$ is a window function centered at t , $\{w(\tau - t)s_1(\tau)\}_\theta$ is a rotated version of $w(\tau - t)s_1(\tau)$ by a constant phase θ . Then, the nonstationary phase rotation can be removed based on equation (4).

Examples

A 0.85s long reflectivity series was calculated from a well log. Figure 1 shows the reflectivity series and its amplitude spectrum. There is an obvious roll-off in the amplitude spectrum from 0 Hz to 100Hz, which indicates that the reflectivity has spectral color (the roll-off for frequencies above 140 Hz is due to an anti-alias filter). The amplitude Gabor spectrum of the reflectivity series is shown in Figure 2. We can see the low amplitude zones around 0.5s and from 0.8s to the end, which means that the color feature of the nonwhite reflectivity is time-variant. In general, the true reflectivity shown in figure 1 has obvious spectral and temporal color.

The true reflectivity was rotated by 60 degrees. The result is shown in figure 3. These two reflectivity series were then used to test our method of measuring nonstationary phase rotation as formulated by equation (5). The measured phase rotation is shown in figure 4. We can see that the measurement is accurate with a relative error less than 1%.

A synthetic attenuated seismic trace was created by applying a forward Q filter to the nonwhite reflectivity, and then convolving the result with a source wavelet. For the examples in this article, the Q value is 50, and the source wavelet is a minimum phase wavelet with a dominant frequency of 40Hz. Conventional Gabor deconvolution and color correction deconvolution were applied to the created seismic trace. The results are shown in figure 5. We can see that conventional Gabor deconvolution gave distorted amplitude estimation from 0.5s to 0.8s compared to the reflectivity, which corresponds to the low magnitude area of the Gabor spectrum shown in Figure 2. With color correction, the estimated result is very close to the true reflectivity. Figure 6 shows the envelopes of the estimated reflectivity and the true reflectivity. The nonstationary phase rotation between estimated reflectivity and true reflectivity are shown in figure 7. The results indicate that the reflectivity color can give rise to distorted amplitude and large phase rotation.

To distinguish the influence of spectral color and temporal color on Gabor deconvolution, we separated these two color features from the Gabor spectrum of the nonwhite reflectivity. For the Gabor amplitude spectrum $|R_G(\tau, f)|$ shown in figure 2, Summation over frequency was conducted to obtain a magnitude estimation for each time sample τ , then the time-variant magnitude was mapped to all frequencies to produced a temporal color addressed version of $|R_G(\tau, f)|$ as shown in figure 8. Dividing the $|R_G(\tau, f)|$ by its' temporal color addressed version

gave a spectral color addressed version shown in figure 9. Color correction was applied separately using the temporal color addressed and spectral color addressed Gabor spectra. The results are shown in figure 10. The spectral color addressed estimation has similar waveform but distorted amplitude compared to the true reflectivity. The temporal color addressed estimation demonstrates close amplitude but different waveform compared to the true reflectivity. A comparison of the envelopes of the estimated reflectivity is shown in figure 11, and figure 12 displays the nonstationary phase rotation between the estimated reflectivity and the true reflectivity. The results reveal that the spectral color and temporal color is the main source of large phase rotation and amplitude distribution respectively.

Conclusions

In practice, the reflectivity is usually nonwhite, often demonstrating obvious spectral color and temporal color. In presence of nonwhite reflectivity, conventional Gabor deconvolution gives a distorted estimation with incorrect relative amplitude and large phase rotation. Color correction can significantly improve the reflectivity estimation for Gabor deconvolution, in particular, testing with synthetic data reveals that the temporal color and spectral color are responsible for amplitude distortion and phase rotation respectively.

Acknowledgements

The authors would like to thank the sponsors of CREWES project, NSERC, POTSI and MITACS for their financial support to this project.

References

- Margrave, G., and Lamoureux, M., 2001, Gabor deconvolution: The CREWES Project Research Report, 13, 241-276.
 Cheng, P., and Margrave, G. F., 2009, Color correction for Gabor deconvolution and nonstationary phase rotation: CSPG CSEG CWLS convention, abstract.

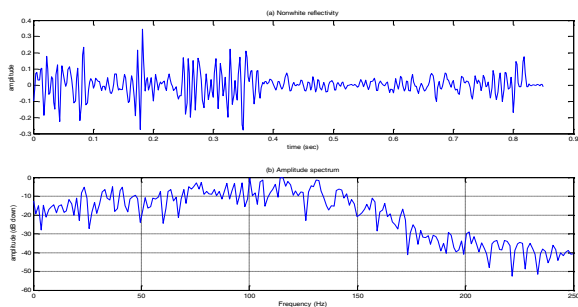


Figure 1. (a) Nonwhite reflectivity calculated from well log. (b) Fourier amplitude spectrum of nonwhite reflectivity.

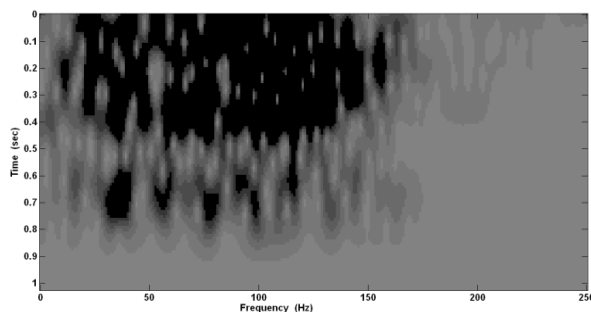


Figure 2. Gabor amplitude spectrum of nonwhite reflectivity shown in figure 1(a).

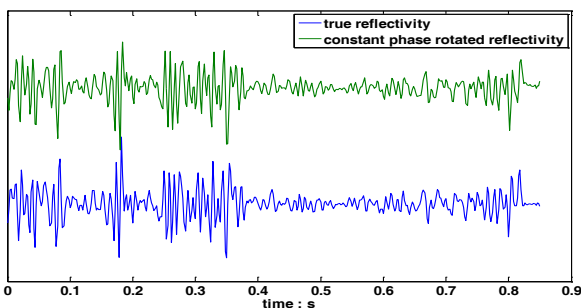


Figure 3. A true reflectivity series and its' 60 degree rotated version

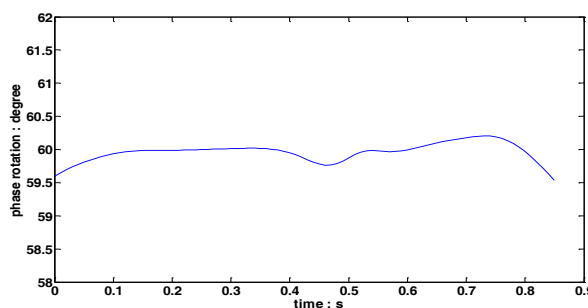


Figure 4. Phase rotation measurement for the two reflectivity series shown in figure 3.

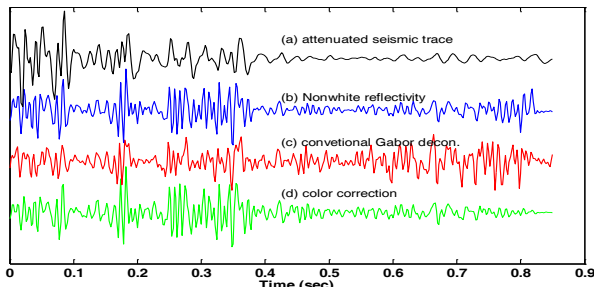


Figure 5. Gabor deconvolution with a frequency band of 10-150 Hz. (a) Nonwhite reflectivity. (b) Synthetic attenuated trace. (c) Gabor deconvolved trace without color correction. (d) Gabor deconvolved trace with color correction using a complete well log.

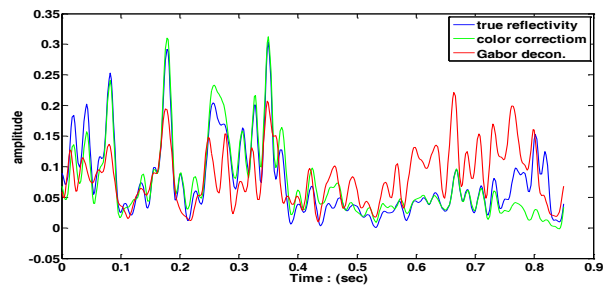


Figure 6. Envelopes of the reflectivity series shown in figure 5.

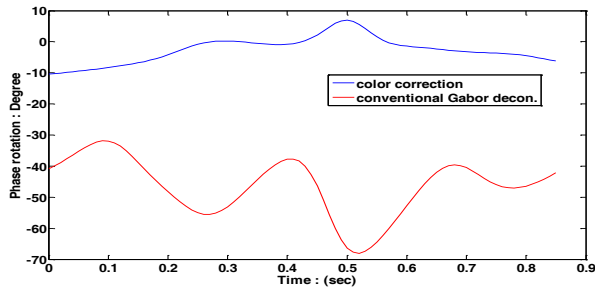


Figure 7. Nonstationary phase rotation of the estimated reflectivity shown in figure 5.

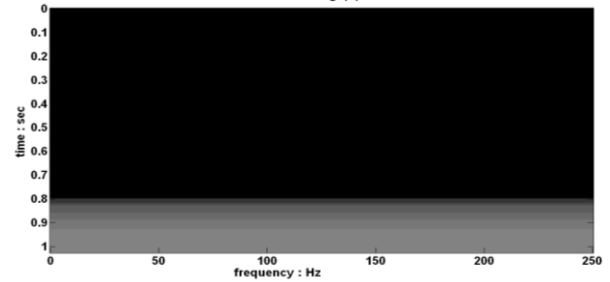


Figure 8. Temporal color of the Gabor spectrum shown in figure 2.

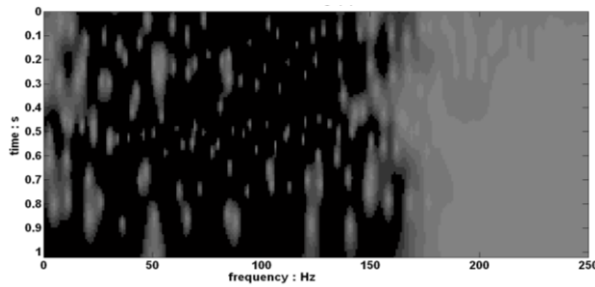


Figure 9. Spectral color of the Gabor spectrum shown in figure 2.

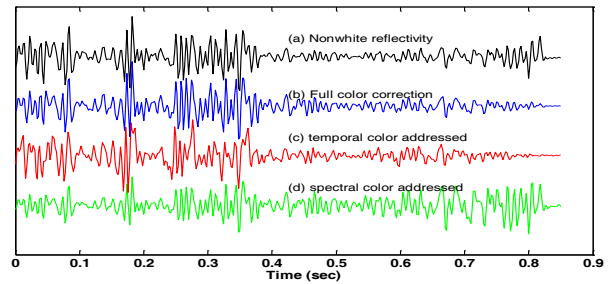


Figure 10. Reflectivity estimations: (a) true reflectivity; (b) full color correction estimation; (c) temporal color addressed estimation; (d) spectral color addressed estimation.

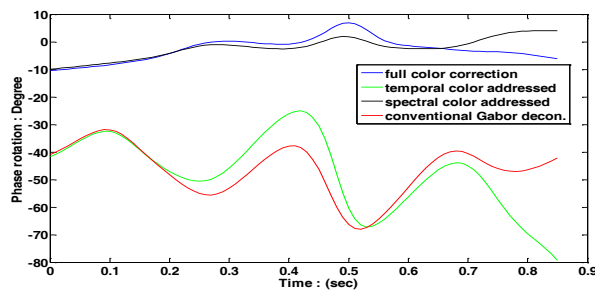


Figure 11. phase rotation of reflectivity estimations shown in figure 10.

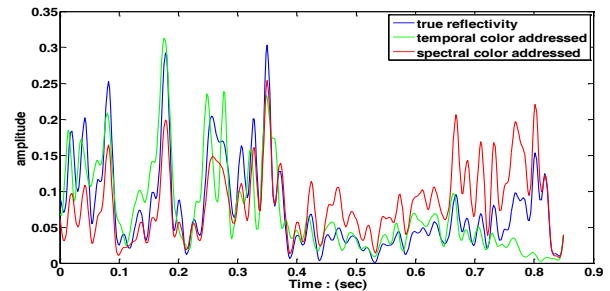


Figure 12. Envelopes of the reflectivity series shown in figure 10.